

Jump Restore Light Transport

SASCHA HOLL, MPI Informatics Saarbrücken, Germany
 HANS-PETER SEIDEL, MPI Informatics Saarbrücken, Germany
 GURPRIT SINGH, MPI Informatics Saarbrücken, Germany

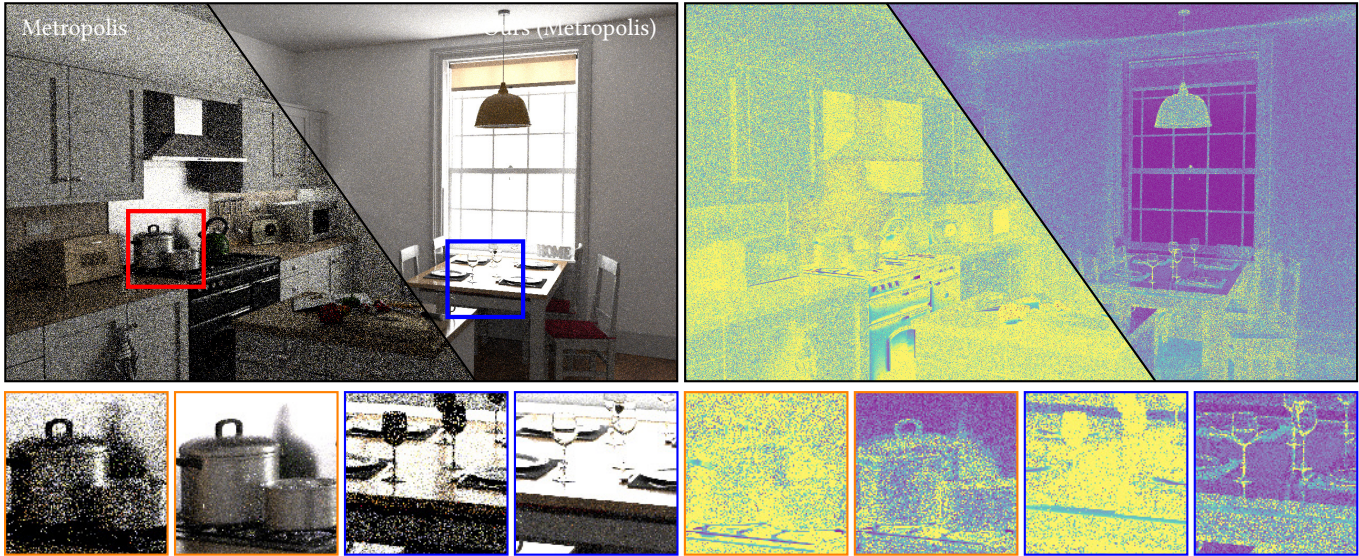


Fig. 1. We introduce a diffusion-based MCMC formulation that subsumes all existing MCMC samplers employed in rendering. We demonstrate the impact on the Metropolis algorithm [Hachisuka et al. 2014] (left) when it is incorporated into our framework (right). The right column is showing the error (MAPE) images. The insets in the bottom row highlights how our method can efficiently handle difficult regions (right-ones are ours).

Markov chain Monte Carlo (MCMC) algorithms come to rescue when sampling from a complex, high-dimensional distribution by a conventional method is intractable. Even though MCMC is a powerful tool, it is also hard to control and tune in practice. Simultaneously achieving both *local exploration* of the state space and *global discovery* of the target distribution is a challenging task. In this work, we present a MCMC formulation that subsumes all existing MCMC samplers employed in rendering. We then present a novel framework for *adjusting* an arbitrary Markov chain, making it exhibit invariance with respect to a specified target distribution.

To showcase the potential of the proposed framework, we focus on a first simple application in light transport simulation. As a by-product, we introduce continuous-time MCMC sampling to the computer graphics community. We show how any existing MCMC-based light transport algorithm can be embedded into our framework. We empirically and theoretically prove that this embedding is superior to running the standalone algorithm. In fact, our

Authors' addresses: Sascha Holl, MPI Informatics Saarbrücken, Saarbrücken, Germany, sholl@mpi-inf.mpg.de; Hans-Peter Seidel, MPI Informatics Saarbrücken, Saarbrücken, Germany, hpseidel@mpi-inf.mpg.de; Gurprit Singh, MPI Informatics Saarbrücken, Saarbrücken, Germany, gsingh@mpi-inf.mpg.de.

Permission to make digital or hard copies of all or part of this work for personal or classroom use is granted without fee provided that copies are not made or distributed for profit or commercial advantage and that copies bear this notice and the full citation on the first page. Copyrights for components of this work owned by others than ACM must be honored. Abstracting with credit is permitted. To copy otherwise, or republish, to post on servers or to redistribute to lists, requires prior specific permission and/or a fee. Request permissions from permissions@acm.org.

© 2024 Association for Computing Machinery.

XXXX-XXXX/2024/9-ART \$15.00

<https://doi.org/10.1145/nmnnnnn.nmnnnnn>

approach will convert any existing algorithm into a highly parallelizable variant with shorter running time, smaller error and less variance.

CCS Concepts: • **Mathematics of computing** → **Markov-chain Monte Carlo methods**; • **Computing methodologies** → **Rendering**.

Additional Key Words and Phrases: Diffusion processes, jump-type Markov processes Markov chain Monte Carlo, light transport simulation

ACM Reference Format:

Sascha Holl, Hans-Peter Seidel, and Gurprit Singh. 2024. Jump Restore Light Transport. 1, 1 (September 2024), 13 pages. <https://doi.org/10.1145/nmnnnnn.nmnnnnn>

1 INTRODUCTION

Creating photo-realistic images necessitates the computation of high-dimensional integrals; typically achieved through Monte Carlo integration. Traditionally, this method amounts to the generation of independent samples within each pixel of the image space. However, a significant drawback of this approach is that samples are generated irrespectively of their contribution to the final estimation. Even when a sample makes no contribution, it is still generated.

Markov chain Monte Carlo (MCMC) can address this insensitivity to the target distribution. By constructing a Markov process, we can guide sample generation to adhere more closely to the target distribution and navigate it through the underlying space in a more controlled manner. Veach and Guibas [1997] introduced Metropolis-Hastings algorithm, an MCMC sampling method, to the rendering

community. The chain constructed by the Ordinary Metropolis-Hastings algorithm is not only invariant, but even reversible with respect to the target distribution.

The invariance property, which is necessary for usage in Monte Carlo sampling, highly restricts our choice of processes, which we can use for state space exploration. That is, even when we have a process at hand, which is able to explore our given state space in a favorable manner, we cannot use it for Monte Carlo sampling, unless it is invariant.

Reversibility is an even stronger condition. While it yields certain useful spectral properties of the process, it also slows down mixing and convergence to equilibrium. Reversible processes show backtracking behavior where the processes frequently revisit previously visited states before reaching unexplored areas, thereby, slowing down the convergence.

Another challenge with designing MCMC algorithms is that the highly correlated Markov chains can cause excessive local exploration which in rendering are visible as overly bright pixels. To avoid this issue, MCMC algorithms should discover other contributing areas by globally discovering the paths away from the current path. All existing algorithms [Veitch and Guibas 1997; Luan et al. 2020a; Li et al. 2015a] are based Metropolis-Hastings which inherits its slower convergence due to the reversibility property.

To overcome the above mentioned issues, we present a novel framework for using an *arbitrary* Markov chain for Monte Carlo sampling from a given target distribution π . That is, we allow to use *any* Markovian state transitioning scheme for state space exploration. In practice, such schemes are usually designed for *local* exploration and are derived from time-discretized diffusion processes.

In our framework, we spawn multiple instances of the chosen Markov chain. Each instance is only executed for a finite amount of time; referred to as the *lifetime* of the instance. *Global discovery* of the whole state space is then ensured by *transferring* execution of the upcoming instance to another, potentially undiscovered portion, of the state space after the lifetime of the previous instance has ended. The transfer description can be designed by the user. We show that the lifetimes can be chosen such that the overall process, defined by this scheme, is π -invariant. That way, this procedure can be seen as *adjusting* a given Markov chain to an π -invariant one. This framework is beneficial for multiple reasons:

- (1) It allows the usage of *any* user-defined Markov chain with the prescribed (local) exploration properties, without the need of worrying about a possibly missing π -invariance;
- (2) it is rejection-free and global discovery is naturally ensured by the transfer mechanism;
- (3) If the spawn location of the next instance under the user-defined transfer description does not depend on the exit point of the previous instance, all processes can be executed in parallel. This is in complete contrast to the Metropolis-Hastings algorithm, which is strictly sequential in its nature.

Outline of this work. We begin our discussion with a brief overview of the general Markov chain Monte Carlo (MCMC) methodology in section 3. Subsequently, in subsection 3.1, we explore the Metropolis-Hastings algorithm, arguably the most

prominent variant of MCMC. The effectiveness of the Metropolis-Hastings algorithm critically depends on the choice of a suitable proposal kernel, which is primarily designed to facilitate rapid local exploration. The most significant choices for these kernels are typically derived from diffusion processes.

To ensure global discovery, small-scale steps must be mixed with large-scale movements. Without the latter, full exploration of multimodal target distributions is not guaranteed. We elaborate on that in section 4.

In section 5, we adopt and slightly extend a novel MCMC-sampler recently proposed in Wang et al. [2021]. It enables a smooth interplay between user-defined local exploration and global discovery. This is achieved by transferring execution to potentially undiscovered portions of the space at a rate that is sensitive to the target distribution.

While we keep an extension for future work, we focus on the *pure jump-type* Markov process scenario already considered in Wang et al. [2021] for our practical setup. A baseline practical implementation is presented in section 6, followed by a numerical study in section 7, where we apply our framework to the light transport problem. We demonstrate how every existing MCMC-based light transport algorithm can be integrated into our framework, resulting in an algorithm that is not only faster but also more accurate. As this represents just the beginning of utilizing our highly general framework, we conclude this paper with a discussion of very promising directions for future research in section 8.

2 RELATED WORK

MCMC in rendering. Physically based rendering algorithms primarily solve the rendering equation [Kajiya 1986] using path tracing algorithms [Pharr et al. 2021]. Bidirectional variants of path tracing (BDPT) [Lafortune and Willems 1996; Veitch and Guibas 1995] are designed to estimate sample paths from both the camera and light source simultaneously, utilizing multiple importance sampling (MIS) estimators. There is one major issue, ordinary Monte Carlo estimators are not able to resolve: samples need to be generated without taking their contribution to the final estimate into account. MCMC rendering algorithms, introduced by Veitch and Guibas [1997], mark the departure from classical Monte Carlo rendering estimators. Various improvements are proposed since then both in the original path space [Cline et al. 2005; Hanika et al. 2015; Kaplanyan et al. 2014] and in the primary sample space [Kelemen et al. 2002]. Bitterli et al. [2017], Pantaleoni [2017], and Otsu et al. [2017] bridge path space and primary sample space with a parametric family of mappings and their inverses.

To better handle local explorations for anisotropic target distributions, Li et al. [2015a] introduced a Hamiltonian Monte Carlo-based MLT algorithm. Their method uses both first and second-order derivatives, together with an HMC-inspired proposal distribution, to generate proposals in primary sample space. Luan et al. [2020a] propose to use only the first-order gradient information to generate high-quality proposals, without the need for expensive second-order differentiation. The dependence on gradients and Hessian computations make these methods computationally expensive. To find a compromise in the computation cost and global and local

exploration, Rioux-Lavoie et al. [2020] propose a two-step mutation strategy in the primary sample space. If the first strategy is rejected, they propose a second strategy using a different proposal distribution. This idea is based on delayed rejection [Tierney and Mira 1999].

Although quite effective, these methods are based on Metropolis-Hastings algorithm to ensure invariance, which inherits reversibility. That is, the process may backtrack and revisit already visited states causing slower convergence towards equilibrium. In this work, we propose a continuous domain formulation which, unlike Metropolis-Hastings, is rejection free and does not require reversibility. Consequently, all generated samples are used towards state exploration and global discovery, giving significantly higher convergence.

MCMC in statistics. The most prominent MCMC algorithm, the Metropolis-Hastings algorithm has been intensively studied. *Optimal scaling* [Roberts and Rosenthal 2001] of Gaussian proposal variances has drawn a lot of attention and several variants like *delayed rejection* [Mira 2011], *multiple-try* [Liu et al. 2000] and *reversible jump* [Green 1995] Metropolis-Hastings algorithms arose from the original attempt. Within the realm of modeling random evolution in diverse dynamical systems [Sharpe 1988], Markov processes emerge as a versatile tool. Dynamical systems exhibiting deterministic outcomes adhere to Ordinary Differential Equations (ODEs), while those characterized by inherent randomness find representation through Stochastic Differential Equations (SDEs). A cornerstone in comprehending randomness within continuous functions is Brownian motion, and the utilization of diffusion processes introduces a wide array of random functions with applications and algorithms spanning various domains. To discretely represent differential equations, the Euler-Maruyama scheme [Kloeden and Platen 1992; Jentzen and Kloeden 2011] stands out as a commonly employed technique. In the context of our work, we base our work on the mathematical framework provided by Wang et al. [2021] to establish the theoretical foundations, thereby delving into the intricate interplay of local and global dynamics of the system under consideration. We propose a highly general framework which makes Wang et al. [2021]’s approach a special case, where state exploration is driven by fixed local dynamics which are spawned from a state-independent regeneration distribution.

3 MARKOV CHAIN MONTE CARLO

Given a finite measure π , Markov chain Monte Carlo (MCMC) is a technique for estimating the integral

$$\pi f := \int f d\pi \quad (1)$$

of a π -integrable function f . More precisely, it is a recipe for constructing an ergodic Markov process with invariant distribution π .

Note that, throughout this work, we use an established operator-theoretic notation to simplify the representation of the mathematical description. In (1), π is treated as an operator acting on the spaces

$$\mathcal{L}^p(\pi) := \{f : f \text{ is } \pi\text{-integrable}\}, \quad (2)$$

where $p \geq 1$.

Table 1. Commonly used notations throughout the document.

Notation	Description
t, x	Time and state at which a process is considered
S	Ergodic average estimator (p. 3)
λ	Reference measure wrt which densities are considered
π	target (probability) distribution
ρ	Density of π wrt λ
X	Overall process (p. 5)
μ	Global dynamics (p. 6) or large step distribution (p. 5) depending on the context
τ	Lifetime of a process (p. 5)
c	Killing rate (p. 5)
M	Local dynamics (5) or Metropolis-Hastings chain (4)
Q	Proposal kernel (p. 4) of the Metropolis-Hastings algorithm
q	Density of Q wrt λ
α	Acceptance function (p. 4) of the Metropolis-Hastings algorithm
$\mathcal{U}_{[0,1]}$	Uniform distribution on $[0, 1)$
$\text{Exp}(\eta)$	Exponential distribution with parameter η

Below, we informally recap the definition of a Markov process and explain when it is called invariant and ergodic. Readers familiar with these concepts may skip directly to section 4 without loss of continuity.

Markov process. A process is a state system evolving over time. In this work, the time domain T will either be discrete, $T = \mathbb{N}_0$, or continuous, $T = [0, \infty)$. Informally, the process is said to be Markov, if at any fixed point in time, the evolution of the process does only depend on the present state, but not on the past.

Invariance. π being an invariant distribution of a Markov process $(X_t)_{t \in T}$ is equivalent to enforcing that once $(X_t)_{t \in T}$ is distributed according to π at a certain time point $s \in T$, every state X_t at a future time point $t \in I \cap (s, \infty)$ will be distributed according to π as well. That is, the distribution of a state is stationary in time after it once coincided with π .

Ergodicity. The ergodicity, on the other hand, will ensure that the long time average of an observation is effectively equal to space averaging with respect to the invariant distribution. That is, given that the invariant distribution π actually exists, ergodicity is equivalent to enforcing

$$S_t f := \frac{1}{t} \left\{ \begin{array}{l} \sum_{s=0}^{t-1} f(X_s) \quad , \text{ if } T = \mathbb{N}_0 \\ \int_0^t f(X_s) ds \quad , \text{ if } T = [0, \infty) \end{array} \right\} \xrightarrow{t \rightarrow \infty} \pi f \quad (3)$$

for all $f \in \mathcal{L}^1(\pi)$. The convergence in (3) holds true \mathbb{P}_π -almost surely. Here, \mathbb{P}_π is a probability measure with respect to which $(X_t)_{t \in T}$ is a Markov process with initial distribution π and the convergence \mathbb{P}_π -almost surely means that

$$(S_t f)(\omega) \xrightarrow{t \rightarrow \infty} \pi f \quad (4)$$

for every outcome ω outside a \mathbb{P}_π -null set.

If $f \in L^p(\pi)$ for some $p \geq 1$, the convergence in (3) also holds true in $L^p(P_\pi)$. That is,

$$\|S_t f - \pi f\|_{L^p(P_\pi)}^p = P_\pi |S_t f - \pi f|^p \xrightarrow{t \rightarrow \infty} 0. \quad (5)$$

Once again, in (5) we are using the operator-theoretic notation $P_\pi |S_t f - \pi f|^p$ to denote the integral of $|S_t f - \pi f|^p$ with respect to the finite measure P_π .

This characterization of ergodicity is known as *Birkhoff's ergodic theorem* [Kallenberg 2021, Theorem 25.6]. In light of (3), it is evident why $(S_t)_{t \in T \setminus \{0\}}$ is usually called the *ergodic average estimator* of π . In this work, we will always assume that the processes under consideration admit this form of ergodicity.

3.1 Metropolis-Hastings algorithm

Arguably the most popular and widely applicable MCMC method is the *Metropolis-Hastings algorithm*. It is an algorithmic construction of a Markov chain $(M_n)_{n \in \mathbb{N}_0}$ with invariant distribution π . The procedure of simulating this chain up to a given time $n \in \mathbb{N}_0$ is summarized in Algorithm 3.1.

Algorithm 3.1 Metropolis-Hastings algorithm with proposal kernel Q and target distribution π .

Input: Initial state x_0 and sample count $n \in \mathbb{N}$.

```

1: procedure METROPOLISHASTINGSUPDATE( $x$ )
2:   Sample  $y$  from  $Q(x, \cdot)$ ; ← generate the proposal
3:   Sample  $u$  from  $\mathcal{U}_{[0, 1]}$ ; ← uniform distribution on  $[0, 1]$ 
4:   if ( $u < \alpha(x, y)$ )
5:     return  $y$ ; ← with probability  $\alpha(x, y)$  return the proposal
6:   return  $x$ ; ← with probability  $1 - \alpha(x, y)$  reject the proposal
7:
8: for ( $i = 1; i < n; ++i$ )
9:    $x_i = \text{METROPOLISHASTINGSUPDATE}(x_{i-1})$ ;
10: return  $(x_0, \dots, x_{n-1})$ 

```

Algorithmic description. The user has to specify a *proposal kernel* Q . For every state x , $Q(x, \cdot)$ is a probability measure. Now, at each discrete time step, the algorithm is *proposing* a state transition candidate y by sampling from $Q(x, \cdot)$, where x is the current state of the chain generated so far. With probability $\alpha(x, y)$, where α is an *acceptance function*, the *proposal* y is *accepted* (line 5) and the current state is set to y . With the opposite probability, $1 - \alpha(x, y)$, the proposal is *rejected* (line 6) and the current state will not be changed (cf. line 9).

Requirements. The initial point x_0 in Algorithm 3.1 can be arbitrary. The only requirement on the proposal kernel Q is that the target distribution π is absolutely continuous with respect to $Q(x, \cdot)$; i.e.

$$\pi(B) = 0 \quad (6)$$

for every state x and $Q(x, \cdot)$ -null set B . Note that this assumption is natural: No matter in which state x the chain is, a proposal from $Q(x, \cdot)$ should be able to reach any region B in which the target distribution π has positive measure.

Acceptance function. The mechanism ensuring that a Markov chain $(M_n)_{n \in \mathbb{N}_0}$ is actually π -invariant is the acceptance/rejection step in Line 5. The acceptance function α cannot be arbitrary, but must be defined in a specific way. There is more than one suitable choice, but the one usually given is optimal with respect to the *Peskun-Tierney ordering* [Tierney 1998]. In order to define it, we are assuming that both, the target distribution π and the proposal kernel Q , admit a density with respect to a common reference measure. That is, we are assuming that

$$p_\lambda := \lambda p \in (0, \infty) \quad (7)$$

and

$$\pi = \frac{p}{p_\lambda} \lambda \quad (8)$$

for some \mathcal{E} -measurable $p : E \rightarrow [0, \infty)$ and a σ -finite measure λ on (E, \mathcal{E}) . And, analogously,

$$Q(x, \cdot) = q(x, \cdot) \lambda \quad \text{for all } x \in E \quad (9)$$

for some $\mathcal{E}^{\otimes 2}$ -measurable $q : E^2 \rightarrow [0, \infty)$. The acceptance function is now defined as

$$\alpha(x, y) := \begin{cases} \min\left(1, \frac{p(y)q(y, x)}{p(x)q(x, y)}\right) & , \text{ if } p(x)q(x, y) > 0 \\ 1 & , \text{ otherwise} \end{cases} \quad (10)$$

DEFINITION 3.1. Algorithm 3.1 with acceptance function (10) and the generated chain $(M_n)_{n \in \mathbb{N}_0}$ are called **Metropolis-Hastings algorithm** and **Metropolis-Hastings chain with proposal kernel Q and target distribution π** , respectively. \square

In practice, we usually do not know the *normalization constant* p_λ , which is the reason why we pulled that value out of the definition of p . Gratefully, as apparent from (10), access to the unnormalized density p is all we need.

Discussion. The choice of the proposal kernel Q has turned out to be crucial to ensure rapid convergence to equilibrium. Various proposal kernels are proposed in rendering [Veach and Guibas 1997; Luan et al. 2020a; Li et al. 2015a], but they all suffer from slower convergence due to the inherent reversible nature of the Metropolis-Hastings algorithm.

4 ENSURING GLOBAL DISCOVERY

There is an additional issue we have not addressed so far. The most common proposal kernels for the Metropolis-Hastings algorithm used in practice, are based on time-discretized diffusion processes. They are excellent for local exploration. However, without incorporation of *large scale movements*, exploration of the whole state space will be slow and could even get stuck in local modes of the target distribution. This is particularly transparent in the (Metropolis-adjusted or not) Langevin algorithm, since it is effectively a stochastically perturbed gradient descent update scheme. One such example is shown in fig. 2. The target distribution shown in black has three modes. We generate 1M (one million) samples shown in orange. Depending on the initial state chosen, only a single mode is discovered. This does not come to a surprise. By (10), the small moves are rejected when the current state is placed (goes) outside of the mode. This is simply due to the rapidly decreasing target density value.

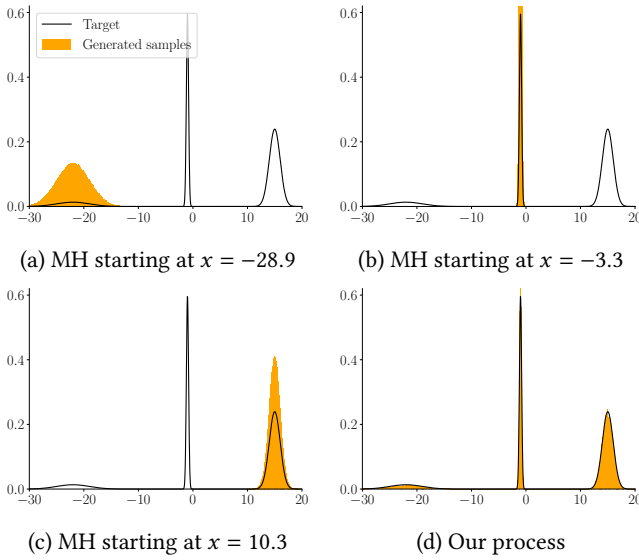


Fig. 2. Existing MCMC methods have difficulty exploring multi-modal distributions. For a given target distribution shown in black we demonstrate this exploration. The explorative nature of Metropolis-Hastings (MH) algorithm is quite restrictive and generate samples nearby the initial sample, initialized near each different mode with variance 1 in (a), (b) and (c). The algorithm only explores the local neighborhood. Our proposed approach (d) improves upon both local exploration and global discovery across all modes.

Mixture proposal. For that reason, in the Metropolis-Hastings algorithm, global discovery can only be ensured by mixing in large scale proposals. That is, a typical proposal kernel Q has the form of a *mixture*:

$$Q_\ell(x, \cdot) := \ell\mu + (1 - \ell)\zeta(x, \cdot) \quad \text{for } x \in E \quad (11)$$

Intuitively, ℓ , μ and ζ are referred to as the *large step probability*, *large step distribution* and *small step kernel* of the proposal scheme, respectively. By construction, $\ell \in [0, 1]$ is controlling the probability of performing a *large step* move according to μ . In order for this to work well, μ should be able to make large jumps across the state space, while ζ should keep exploring local neighborhoods.

Practical limitations. Even though this attempt works pretty well in practice, it is hard to give a general choice for the large step probability ℓ . Not only that, according to (11) a *large step proposal* is proposing a large scale move *uniformly*. That is, the proposal is made without knowledge of how productive the current phase of the exploration is. Even though it can be rejected when the target density at the proposed state is significantly smaller than at the current state, there is a potential of drawing the exploration away from a region where the exploration was going on well. Not only that, upon rejection the chain will be remain in the previous state, which will slow down the speed of exploration.

The sampler constructed in this work will address this issue. In some sense, it will yield *rejection-free* global moves, which are happening on a rate sensitive to the shape of π in the region explored before the move.

5 THE JUMP RESTORE ALGORITHM

In this section, we present a slightly extended version of the *jump Restore algorithm* proposed in Wang et al. [2021]. We also formulate the framework with less restrictive assumptions on the target distribution and stress that correctness still can be proven rigorously.

Basic idea. The core idea is to simulate a Markov chain that explores the space locally, terminating this simulation after a finite amount of time, and then restarting it at a different location in the space. We refer to a single simulation of the Markov chain, up to the point of termination, as a *tour*. The termination point is determined based on the elapsed runtime and the target density at the current position of the simulation. After the termination of a tour, a new instance of the Markov chain is spawned at a new location in space. This process is referred to as a *transfer* of the simulation. The last state of the previous instance is called *exit point* while the starting point of the new instance is called *spawn location*. The latter can be chosen based on the previous exit point.

Ensuring invariance. First, we choose a Markov chain M constituting the *local dynamics* of the overall process. That is, we choose a Markov chain M that is (at least conceptually) well-suited for *local* exploration of our state space. We then spawn instances M^i of M at various locations in the space.

To ensure that our algorithm is invariant with respect to a given target distribution π and to prevent the individual instances from becoming trapped in local modes of π after some time, we restrict the simulation of M^i to a time τ_i , immediately before which we terminate the simulation of M^i . This time τ_i is referred to as the *lifetime* of M^i .

Lifetime choice. It turns out that the appropriate choice for τ_i is the one which is determined by a clock that decays with a suitable time-dependent exponential rate. To give meaning to this description, we must interpret M as a continuous-time process. We achieve this by holding each state M_{n-1} for an exponentially distributed amount of time before transitioning to M_n according to $\zeta(M_{n-1}, \cdot)$. To avoid altering the asymptotic distribution of M under this *embedding* in continuous time, we choose the parameter of the exponential holding times to be 1. In the sequel, M^i always refers to instances of the continuous-time embedding of M .

We now choose τ_i as the clock that decays at the time-dependent exponential rate

$$[0, \infty) \ni t \mapsto c(M_t^i).$$

The function c is referred to, for obvious reasons, as a *killing rate*.

The overall process. Formally, we execute the instances M^i in sequential order, so that our algorithm, in its entirety, simulates the process

$$X_t = M_{t - \sigma_{i-1}}^i \Leftrightarrow t \in [\sigma_{i-1}, \sigma_i), \quad (12)$$

where

$$\sigma_j := \sum_{i=1}^j \tau_i \quad (13)$$

is the time elapsed after the j th process has been executed.

Transfer of execution. For the first instance M^1 , we choose an initial distribution μ_0 such that M_0^1 is distributed according to μ_0 . For all subsequent instances, we select a family of distributions $\mu(x, \cdot)$, where x is an arbitrary point in the state space, such that M_0^{i+1} is distributed according to $\mu(M_{\tau_i-}^i, \cdot)$. Here,

$$M_{\tau_i-}^i := \lim_{t \rightarrow \tau_i-} M_t^i \quad (14)$$

denotes the *exit point* of the previously executed instance M^i . Since μ describes the transfer of execution from one tour the subsequent one, it constitutes the *global dynamics* of the overall process.

Killing rate. To state the definition for c , we need to assume that the target distribution π has a density p with respect to a reference measure λ . We do not require that p is normalized, but pull the normalization constant

$$p_\lambda := \lambda p \quad (15)$$

out of the definition of p . That is,

$$\pi = \frac{p}{p_\lambda} \lambda. \quad (16)$$

It now turns out that the choice of c that ensures X is invariant with respect to a given target distribution π is

$$c = \frac{(c_0 \mu^* + L^*)p}{p} \quad \text{on } \{ p > 0 \} \quad (17)$$

$$c = \infty \quad \text{on } \{ p = 0 \} \quad (18)$$

for some $c_0 > 0$ large enough to ensure $c \geq 0$. Here,

$$Lf := \zeta f - f, \quad (19)$$

for bounded measurable functions f , denotes the *generator* of the Markov chain M . With μ^* (and, analogously, with L^*) we denote the *adjoint* of μ with respect to the *duality bracket*

$$\langle f, g \rangle_\lambda := \lambda(fg) \quad (20)$$

defined for bounded measurable functions f and $g \in L^1(\lambda)$. That is, μ^* (and, analogously, for L^*) is the unique operator satisfying

$$\langle \mu f, g \rangle_\lambda = \langle f, \mu^* g \rangle_\lambda \quad (21)$$

for all bounded measurable functions f and $g \in L^1(\lambda)$.

It can be shown that the constant c_0 is the "expected lifetime" of a single tour. Optimization of this constant is part of future work (section 8). Also, in Wang et al. [2021] it has been proven that the process X is π -invariant when the killing rate is chosen according to (17). However, the proof given there is making superfluous assumptions, which are usually not satisfied in the applications we are interested in. While a formal proof is outside of the scope of this work, we stress that everything can be proven in the generality given here.

Killing rate for invariant local dynamics. A significant simplification occurs when the Markov chain M is already invariant with respect to the target distribution π . In that case, $L^*p = 0$ and hence (17) simplifies to

$$c = c_0 \frac{\mu^* p}{p} \quad \text{on } \{ p > 0 \}. \quad (22)$$

Killing rate for state-independent global dynamics. Another important simplification can be made, when the distribution μ is state-independent (i.e. when μ is an ordinary probability measure) and has a density u with respect to λ . Once again, we do not require that u is normalized and denote the normalization constant by u_λ . In that case,

$$\mu^* g = (\lambda g) \frac{u}{u_\lambda} \quad \text{for all } g \in \mathcal{L}^1(\lambda). \quad (23)$$

If μ is state-independent and the Markov chain M is already invariant with respect to the target distribution π , (17) simplifies to

$$c = c_0 \frac{p_\lambda u}{u_\lambda p} \quad \text{on } \{ p > 0 \}. \quad (24)$$

The algorithm that implements the entire procedure can be found in Algorithm 5.1. In the sequel, we will refer to it as the *Jump Restore algorithm with local dynamics M and regeneration distribution μ* .

Algorithm 5.1 Jump Restore algorithm

Input: Initial state x_0 and sample count $n \in \mathbb{N}$.

```

1: for ( $i = 1; ++i$ )
2: {
3:   Sample  $t_1$  from  $\text{Exp}(1)$ ;
4:   Sample  $t_2$  from  $\text{Exp}(c(x_{i-1}))$ ;            $\leftarrow \text{Exp}(0) := \delta_\infty$ 
5:   if ( $t_1 < t_2$ )
6:   {
7:      $\Delta t_i = t_1$ ;
8:     if ( $i == n$ )
9:       return ( $(\Delta t_1, x_0), \dots, (\Delta t_n, x_{n-1})$ );
10:    Sample  $x_i$  from  $\zeta(x_{i-1}, \cdot)$ ;
11:  }
12:  else
13:  {
14:     $\Delta t_i = t_2$ ;
15:    if ( $i == n$ )
16:      return ( $(\Delta t_1, x_0), \dots, (\Delta t_n, x_{n-1})$ );
17:    Sample  $x_i$  from  $\mu(x_{i-1}, \cdot)$ ;
18:  }
19: }
```

In each iteration i of Algorithm 5.1, given the current state x_{i-1} , we first sample the holding time t_1 of this state in Line 3. This is the time we would hold the state x_{i-1} before the next (local) state transition according to the Markov chain M would happen. However, before we can perform this transition, we need to make sure that the current tour will not be terminated before this holding time has elapsed. To check for that, we draw another time t_2 from an exponential distribution with rate given by the killing rate $c(x_{i-1})$ at the current state x_{i-1} in Line 4.

If $t_1 < t_2$, which is checked for in Line 5, the ongoing tour is not killed before the next (local) state transition. In that case, we set the time delta δt_i to be the holding time t_1 and, if this iteration is not the last one requested (Line 8), we perform the state transition according to M in Line 10.

If $t_1 \geq t_2$, the ongoing tour is killed before the next (local) state transition would happen. In that case, we set the time delta δt_i to be the time t_2 until the tour is terminated. Unless this iteration is the last one requested (Line 15), we sample the spawn location of the next tour in Line 17.

The output of Algorithm 5.1 can be used to approximate πf for a given (set of) $f \in \mathcal{L}^1(\pi)$. According to (3),

$$\left(\sum_{i=1}^n \Delta t_i \right)^{-1} \sum_{i=1}^n \Delta t_i f(x_{i-1}) \approx \pi f \quad (25)$$

for large enough n .

The jump Restore algorithm combines local exploration of the target density with global exploration of the entire space. Both is achieved by the novel killing and transfer mechanisms. In section section 7, we compare the performance of this attempt to the established method of dealing with global discovery in the Metropolis-Hastings algorithm.

6 PRACTICAL SETUP

For our practical setup, we show how the jump Restore algorithm can accelerate *any* existing MCMC-based light transport algorithm. Without loss of generality, we will assume that the reference algorithm is based on the Metropolis-Hastings algorithm with a mixture proposal kernel.

The reference algorithm. For that reason, given a probability measure π , we denote the Metropolis-Hastings chain with the mixture proposal kernel

$$Q_\ell(x, \cdot) := \ell \mu + (1 - \ell) \zeta(x, \cdot) \quad \text{for } x \in E \quad (26)$$

and target distribution π considered in section 4 by M^ℓ . As in section 4, $\ell \in [0, 1]$, μ is a large step distribution and $\zeta(x, \cdot)$ is a small step distribution for every state x .

The corresponding jump Restore algorithm for comparison. We will now compare the performance of this Metropolis-Hastings algorithm with the jump Restore algorithm with local dynamics M^0 and regeneration distribution μ described in section 5.

That is, the local dynamics we are considering now are given by the Metropolis-Hastings algorithm with a proposal kernel, which (conceptually and also in our numerical study) solely consists of the small step proposals given by ζ . Note that this is the natural usage of the jump Restore algorithm, since the global movements are already incorporated in terms of the regeneration mechanism.

As the present regeneration distribution μ is state-independent, algorithm Algorithm 5.1 is highly parallelizable. Especially given that the lifetimes of the tours are quite short. We can simulate as many tours in parallel as our underlying hardware allows and accumulate the result. The algorithm, which samples from a single tour only, is given in Algorithm 6.1.

While the Metropolis-Hastings algorithm is suffering from burn-in issues (i.e. it may need a long time to travel to the relevant support of the target distribution), the jump Restore algorithm does not. This is by design, since tours spawned at a location beyond the tails of the target distribution get killed immediately.

Algorithm 6.1 Jump Restore algorithm (parallelizable version)

```

1: Sample  $x_0$  from  $\mu$ ;
2: for ( $i = 1; ++i$ )
3: {
4:   Sample  $t_1$  from  $\text{Exp}(1)$ ;
5:   Sample  $t_2$  from  $\text{Exp}(c(x_{i-1}))$ ;            $\leftarrow \text{Exp}(0) := \delta_\infty$ 
6:   if ( $t_1 < t_2$ )
7:   {
8:      $\Delta t_i = t_1$ ;
9:     Sample  $x_i$  from  $\zeta(x_{i-1}, \cdot)$ ;
10:  }
11:  else
12:  {
13:     $\Delta t_i = t_2$ ;
14:    return ( $(\Delta t_1, x_0), \dots, (\Delta t_i, x_{i-1})$ );
15:  }
16: }
```

In section 7, we empirically compare this jump Restore algorithm with the Markov chain M^ℓ . As it will turn out, ensuring global discovery by the regeneration mechanism is superior to relying on the large scale proposals affected by (26). We can even prove this theoretically as we will do in the next section. A theoretical convergence analysis can be found in Appendix A.

7 NUMERICAL STUDY

For our numerical study, we consider the light transport problem. The foundation of MCMC-based light transport simulation goes back to the seminal work [Veach 1997]. Therein, a *path integral formulation* of the light transport problem was given. Due to the generality of our framework, there is no need to rephrase that formulation here.

All of the MCMC-based light transport algorithms, known to date, are Metropolis-Hastings variants (cf. section 2). Specifically, every rendering algorithm we consider now is a Metropolis-Hastings algorithm with a proposal kernel of the mixture form (26). Consequently, we are in the setting described in section 6.

7.1 Rendering environment

We have implemented our approach in the rendering system *pbrt* [Pharr et al. 2023] described in [Pharr et al. 2021]. Therein an implementation of the *multiplexed Metropolis light transport* algorithm, proposed in [Hachisuka et al. 2014], is available. For simplicity, we will refer to this implementation and the corresponding jump Restore algorithm as *Metropolis* and *Ours (Metropolis)*, respectively.

We also implemented our algorithm in the rendering system *dpt* [Li et al. 2015b], which shipped together with [Li et al. 2015a]. The latter is using a proposal kernel Q based on Hamiltonian Monte Carlo (HMC). We will refer to this implementation and the corresponding jump Restore algorithm as *HMC* and *Ours (HMC)*, respectively. Similar, [Luan et al. 2020a] is a variant of the Metropolis-adjusted Langevin algorithm (MALA) and was implemented in [Luan et al. 2020b]. The latter is an extension of the code base [Li

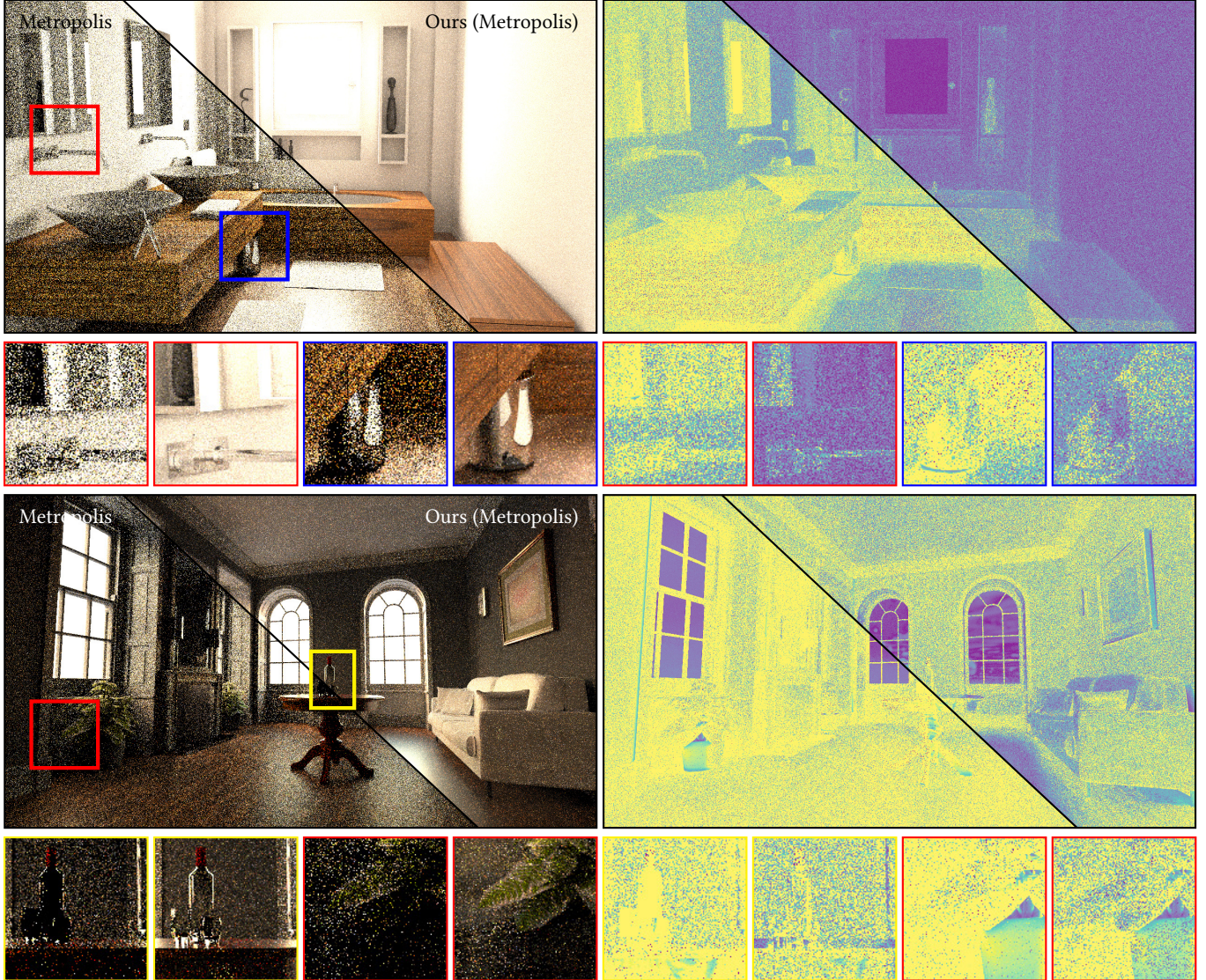


Fig. 3. We perform equal-time comparison of the Metropolis algorithm [Hachisuka et al. 2014] within our proposed framework, we render the BATHROOM scene (top) and the GREY & WHITE ROOM scenes (bottom). Our framework allows extensive parallelism and avoids any rejection sampling, thereby converging much faster towards the reference. All renderings are shown after 20 seconds of the rendering time. For each scene, we also show the error (MAPE) images in the right column. The insets highlight that our approach (the right image in the inset pair) can also handle difficult cases (glass bottle, specular highlights) efficiently.

et al. 2015b]. We refer to this implementation and the corresponding jump Restore algorithm as *MALA* and *Ours (MALA)*, respectively.

7.2 Implementation details

Directly working with the path space description given in [Veach 1997] is hard. Today, almost every approach is working on the so-called *primary sample space* $[0, 1)^d$, where $d \in \mathbb{N}$, instead. This space has been first considered by [Kelemen et al. 2002]. The generated chain is then transformed to the path space. The reason is obvious: $[0, 1)^d$ is easier to work with. In particular, it is way easier to come

up with a sensible choice for the kernel ζ . For that reason, we are effectively working on $[0, 1)^d$. The space $[0, 1)^d$ is considered with a toroidal boundary here.

On this space, the mixture proposal Q_ℓ in Metropolis, HMC and MALA is always of the precisely form

$$Q_\ell(x, \cdot) = \ell \mathcal{U}_{[0, 1)^d} + (1 - \ell) \mathcal{N}_{\zeta \text{id}_{\mathbb{R}^d}}(b(x), \cdot) \quad (27)$$

for all $x \in [0, 1)^d$, where b is some drift and $\zeta > 0$ is controlling the variance of the Gaussian small step kernel.

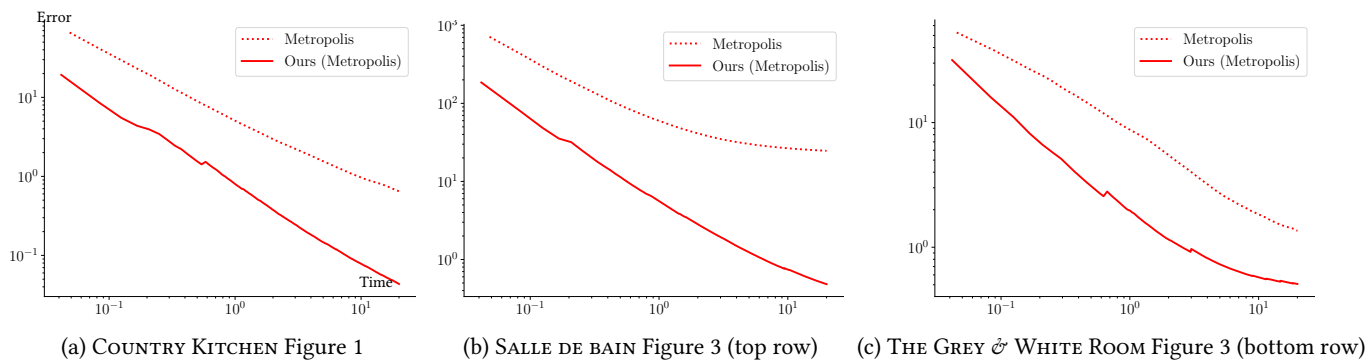


Fig. 4. Convergence plots showing MSE vs. time for different rendering scenes. Our sampler consistently outperformed over time.

For the Gaussian variance parameter, occurring in (27), We specifically choose $\zeta = .01$ which is a practically proven good value for the given setting. As discussed in the last paragraph of section 4, a large step proposal caused by the specific form of \tilde{Q} is an uninformed move, which can practically draw the exploration away from a region of great discovery. Since it is not possible to come up with a generally satisfying choice for the large step probability ℓ , we set it to $.3$, which is a common default. Also, in lack of a better choice, μ is chosen to be the uniform distribution on $[0, 1]^d$. Since are using the local dynamics given by the Metropolis-Hastings chain M^0 and this Markov chain is already invariant with respect to the target distribution π , we can use the simplified definition (24) of the killing rate. The constant c_0 occurring there is chosen to be 1 . An optimization of this choice is part of future work (section 8). Guidance for different choices can be drawn from the interpretation of c_0 as the "expected lifetime" of a single tour and Appendix A.

Since the distribution μ is state-independent, we can effectively run as many instances of Algorithm 6.1 in parallel as possible in order to compute the estimates (25). However, we are limited by the maximal number of concurrent threads supported by our hardware (see section 7.2).

In order to ensure a fair comparison, we also spawned 1000 instances of the Metropolis-Hastings algorithms. As long as the sample count of each chain is long enough, the combination of independent chains in estimation is not an issue. But we stress at this point that the number of simulated independent chains cannot be arbitrary high, since then the chains will suffer from *burn-in issues* [Roberts and Rosenthal 2004].

On the other hand, the restore process has no such limitation. It cannot suffer from burn-in, since - by construction - tour spawn locations beyond the tails of the target distribution are *immediately* killed and hence do not contribute to the estimate at all.

Rendering setup. We run our renderings on a AMD EPYC 7702 64-Core Processor with 64 cores and a clock speed of 2-3.3 GHz. Everything was executed solely on the CPU. Since our hardware limited us to a maximal number of 256 concurrent threads, the results shown in subsection 7.3 will further improve if a higher number of threads can run concurrently on the hardware of the reader.

7.3 Experiments

In an interactive viewer, provided in the supplementary of this work, the reader can investigate the results of our comparison for four different scenes in *pbrt* (SALLE DE BAIN, COUNTRY KITCHEN, THE GREY & WHITE ROOM and THE WOODEN STAIRCASE; all taken from [Bitterli 2016]) and two different scenes in *dpt* (VEACH AJAR DOOR and TORUS, which shipped with [Li et al. 2015a]). In that viewer, the scenes can be view at all samples per pixel counts of 2^k , ranging from $k = 0$ to 10 . Since one of the main advantages of the restore process, compared to the Metropolis-Hastings algorithm, is its parallelizability, we consider *almost* equal time comparisons in this article itself. We say *almost*, cause a *fair* equal time comparison is hard to achieve without compromising one of the compared algorithms. The reason is the completely different nature of the continuous-time sampling approach proposed in this work. Most of the existing equal time comparisons were able to compare different *discrete time* sampling techniques. They were either ordinary Monte Carlo methods or Metropolis-Hastings algorithms. For them, it is easy to obtain a fair comparison by choosing a fixed common thread count. The restore process, on the other hand, can run as many threads in parallel as your hardware allows. Since this procedure needs to stop at a time, where the lifetime of a single tour has been added, we might slightly overshoot a given sample count; which is the cause of the deviating timings. To obtain a fair comparison in the present setting, we parallelized the Metropolis-Hastings variants in the aforementioned manner. Since the timings are not exactly the same, we always penalized ourselves and let the Metropolis-Hastings variant run for *at least* the same time (effectively, for a *longer* time) then the corresponding restore version.

Metropolis vs Ours (Metropolis). The scene COUNTRY KITCHEN depicted in Figure 1 was rendered in *pbrt*. The left- and right-hand sides of the split show the result after 20 seconds of computation time of the Metropolis and Metropolis Restore algorithms, respectively. Metropolis Restore is referred as Ours (Metropolis) in all figures. The pots on the kitchen stove are still quite noisy in the Metropolis result, whereas the Metropolis Restore looks much cleaner. Also, the glasses on the kitchen table have not been fully discovered by Metropolis. These observations are also reflected in the convergence plot Figure 4.

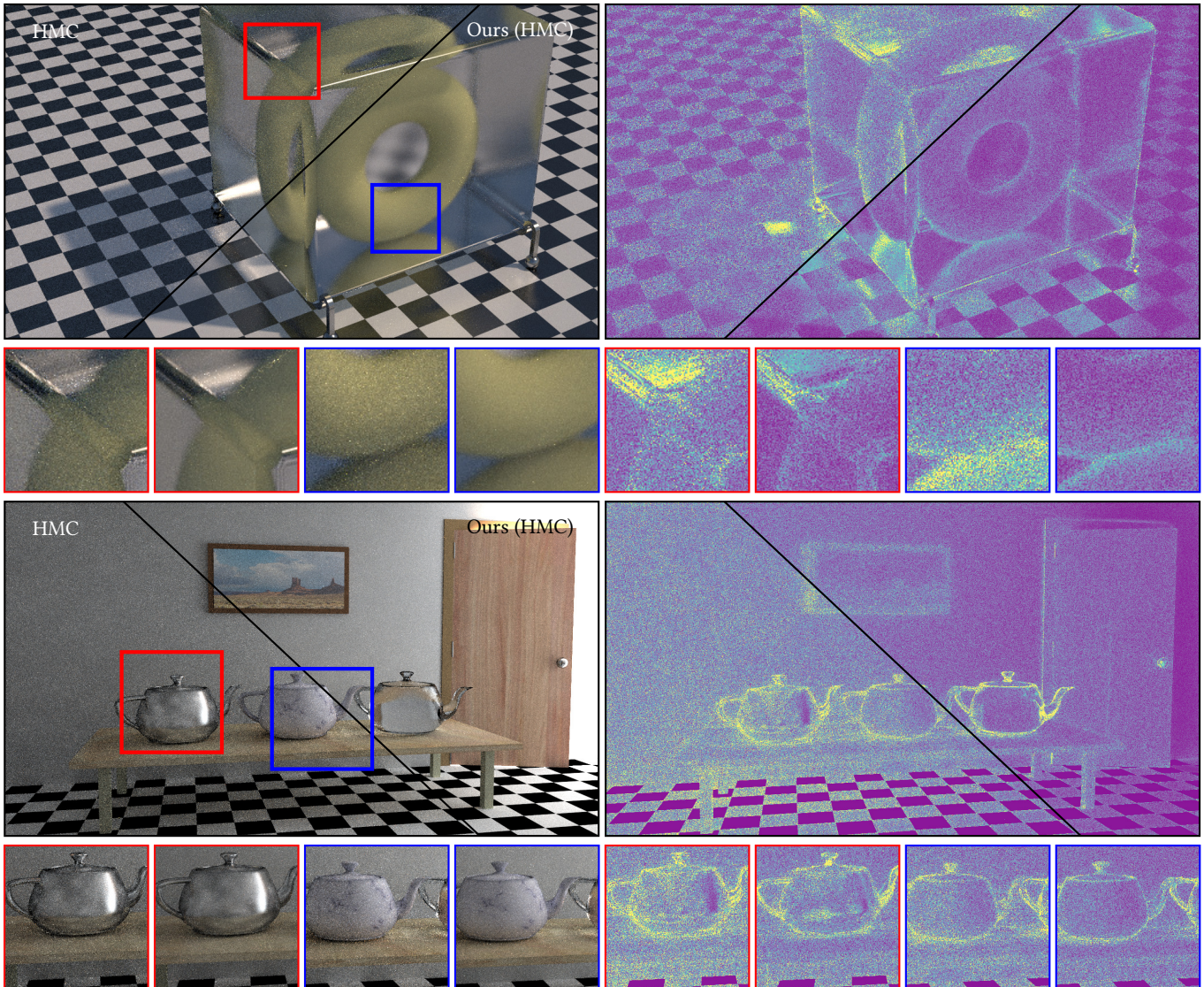


Fig. 5. To compare (equal-time) the HMC algorithm [Li et al. 2015a] within our proposed framework, we render the TORUS scenes (top) and the VEACH DOOR scene (bottom). HMC needs both first and second-order gradients which slows it down. However, with our framework, Ours (HMC) explores the global distribution in a much better way. All renderings are shown after 20 seconds of the rendering time, with error (MAPE) images shown in the right column.

In Figure 3, the BATHROOM and the GREY & WHITE ROOM scenes are also rendered in pbrt. Metropolis Restore (Ours) show consistently improved results compared to Metropolis. The specular highlights in the bathroom scene are better handled by Ours. The wine bottle and the glasses placed in the middle of the room (bottom row) still appear dark when using Metropolis. Ours, on the other hand, explore these regions quite effectively. The convergence plots in fig. 4 shows our Metropolis Restore consistently outperforms Metropolis by a significant margin.

MALA/HMC vs Ours (MALA/HMC). Figure 5 and 7 show the TORUS and VEACHDOOR scene that are rendered using the differentiable path tracer from Li et al. [2015a]; Luan et al. [2020a], respectively. The corresponding convergence plots are shown in fig. 6. The improvements visible using MALA and HMC are mainly due to the better global discovery thanks to our rejection free formulation of the MCMC sampler. The convergence plots for the VEACHDOOR scene shows ours methods as solid lines, whereas the MALA/HMC/Metropolis are shown as dotted lines. Ours show consistent improvements over time.

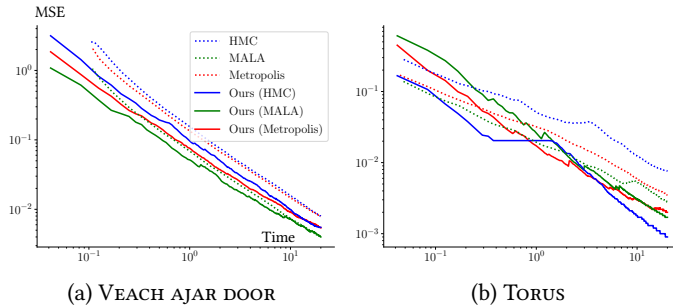


Fig. 6. Convergence plots showing MSE vs. time for different rendering scenes shown in figs. 5 and 7. Our sampler consistently outperformed over time.

8 FUTURE WORK

We introduced a novel framework for adjusting an arbitrary Markov chain for Monte Carlo integration to the graphics community. Especially, we introduced a rejection-free and target density sensitive way to deal with global discovery. We slightly generalized the idea presented in [Wang et al. 2021] and enriched it with an empirical (section 7) and theoretical (Appendix A) convergence analysis.

Research and numerical investigation can continue in many directions from here. First of all, the constant c_0 in (17) has the interpretation of being the "expected lifetime" of a single tour. In lack of a theoretical optimality condition, We have set it to 1. A dedicated variance analysis can be used to try to derive an optimal value for it.

In the same spirit, multiplexed Metropolis Light transport, proposed in [Hachisuka et al. 2014], does still use the choice of weights given by the *balance heuristic* derived in [Veach 1997]. This choice is only (sub-)optimal for the variance of the multiple importance sampling estimator. It is not known to be optimal for the ergodic average estimator corresponding to the Metropolis-Hastings chain. This fact was not mentioned in the literature yet. We now have an additional estimator given by Equation 25. We could again ask what an optimal choice of weights would be. Once again, a dedicated variance analysis can be used to come up with such a derivation.

Next, we could drop the assumption that the regeneration distribution μ is state-independent. Instead, the revival point could be smartly chosen by knowledge of the exit point from the previous tour.

Lastly, and most obviously, different local dynamics could be investigated. For example, instead of considering MALA, one could simulate the Langevin dynamics as they are. Either by an appropriate exact sampling technique or by applying the unadjusted Langevin algorithm. In the latter case, the adjoint term L^*p does not vanish anymore. This yields a new challenge of computing that quantity efficiently.

Given the surge in generative models, our work establishes a solid foundational framework that can be leveraged to establish direct connections between diffusion models [Sohl-Dickstein et al. 2015; Ho et al. 2020] in generative AI, physically based rendering and SGD-based optimization algorithms [Chen et al. 2016].

REFERENCES

- Christophe Andrieu and Samuel Livingstone. 2019. Peskun-Tierney ordering for Markov chain and process Monte Carlo: beyond the reversible scenario. (2019). arXiv:1906.06197
- Benedikt Bitterli. 2016. Rendering resources. <https://benedikt-bitterli.me/resources/>.
- Benedikt Bitterli, Wenzel Jakob, Jan Novák, and Wojciech Jarosz. 2017. Reversible Jump Metropolis Light Transport Using Inverse Mappings. *ACM Trans. Graph.* 37, 1, Article 1 (oct 2017), 12 pages. <https://doi.org/10.1145/3132704>
- Changyou Chen, David Carlson, Zhe Gan, Chunyuan Li, and Lawrence Carin. 2016. Bridging the Gap between Stochastic Gradient MCMC and Stochastic Optimization. In *Proceedings of the 19th International Conference on Artificial Intelligence and Statistics (Proceedings of Machine Learning Research, Vol. 51)*, Arthur Gretton and Christian C. Robert (Eds.). PMLR, Cadiz, Spain, 1051–1060. <https://proceedings.mlr.press/v51/chen16c.html>
- David Cline, Justin Talbot, and Parris Egbert. 2005. Energy Redistribution Path Tracing. *ACM Trans. Graph.* 24, 3 (jul 2005), 1186–1195. <https://doi.org/10.1145/1073204.1073330>
- Andreas Eberle and Francis Lörler. 2024. Non-reversible lifts of reversible diffusion processes and relaxation times. (2024). arXiv:2402.05041
- P.J. Green. 1995. Reversible Jump Markov Chain Monte Carlo Computation and Bayesian Model Determination. *Biometrika* 82, 4 (1995).
- Toshiya Hachisuka, Anton S. Kaplanyan, and Carsten Dachsbacher. 2014. Multiplexed Metropolis Light Transport. *ACM Transactions on Graphics* 33, 4 (2014).
- Johannes Hanika, Anton Kaplanyan, and Carsten Dachsbacher. 2015. Improved Half Vector Space Light Transport. *Computer Graphics Forum* 34, 4 (2015), 65–74. <https://doi.org/10.1111/cgf.12679> arXiv:<https://onlinelibrary.wiley.com/doi/pdf/10.1111/cgf.12679>
- Jonathan Ho, Ajay Jain, and Pieter Abbeel. 2020. Denoising diffusion probabilistic models. *Advances in neural information processing systems* 33 (2020), 6840–6851.
- Arnulf Jentzen and Peter E. Kloeden. 2011. *Taylor Approximations for Stochastic Partial Differential Equations*. Society for Industrial and Applied Mathematics.
- James T. Kajiya. 1986. The rendering equation. *SIGGRAPH Comput. Graph.* 20, 4 (aug 1986), 143–150. <https://doi.org/10.1145/15886.15902>
- Olav Kallenberg. 2021. *Foundations of Modern Probability* (3 ed.). Springer Nature Switzerland AG 2021.
- Anton S. Kaplanyan, Johannes Hanika, and Carsten Dachsbacher. 2014. The natural-constraint representation of the path space for efficient light transport simulation. *ACM Trans. Graph.* 33, 4, Article 102 (jul 2014), 13 pages. <https://doi.org/10.1145/2601097.2601108>
- Csaba Kelemen, László Szirmay-Kalos, György Antal, and Ferenc Csonka. 2002. A Simple and Robust Mutation Strategy for the Metropolis Light Transport Algorithm. *Computer Graphics Forum* 21, 3 (2002), 531–540. <https://doi.org/10.1111/1467-8659.t01-1-00703> arXiv:<https://onlinelibrary.wiley.com/doi/pdf/10.1111/1467-8659.t01-1-00703>
- P.E. Kloeden and E. Platen. 1992. *Numerical Solution of Stochastic Differential Equations*. Springer Berlin Heidelberg. <https://books.google.de/books?id=BCvtssom1CMC>
- Eric P. LaFortune and Yves D. Willems. 1996. Rendering Participating Media with Bidirectional Path Tracing. In *Rendering Techniques '96*, Xavier Pueyo and Peter Schröder (Eds.). Springer Vienna, Vienna, 91–100.
- Tzu-Mao Li, Jaakko Lehtinen, Ravi Ramamoorthi, Wenzel Jakob, and Frédo Durand. 2015a. Anisotropic Gaussian Mutations for Metropolis Light Transport through Hessian-Hamiltonian Dynamics. *ACM Transactions on Graphics* 34, 6 (2015).
- Tzu-Mao Li, Jaakko Lehtinen, Ravi Ramamoorthi, Wenzel Jakob, and Frédo Durand. 2015b. *dpt*. <https://github.com/BachLi/dpt>
- J. S. Liu, F. Liang, and W. H. Wong. 2000. The multiple-try method and local optimization in Metropolis sampling. *J. Amer. Statist. Assoc.* 95, 449 (2000).
- Fujun Luan, Shuang Zhao, Kavita Bala, and Ioannis Gkioulekas. 2020a. Langevin Monte Carlo Rendering with Gradient-based Adaptation. *ACM Transactions on Graphics* 39, 4 (2020).
- Fujun Luan, Shuang Zhao, Kavita Bala, and Ioannis Gkioulekas. 2020b. *lmc*. <https://github.com/luanfujun/Langevin-MCMC>
- Antonietta Mira. 2011. On Metropolis-Hastings algorithms with delayed rejection. *Journal of Statistics* (2011).
- Hisanari Otsu, Anton S. Kaplanyan, Johannes Hanika, Carsten Dachsbacher, and Toshiya Hachisuka. 2017. Fusing state spaces for markov chain Monte Carlo rendering. *ACM Trans. Graph.* 36, 4, Article 74 (jul 2017), 10 pages. <https://doi.org/10.1145/3072959.3073691>
- Jacopo Pantaleoni. 2017. Charted metropolis light transport. *ACM Trans. Graph.* 36, 4, Article 75 (jul 2017), 14 pages. <https://doi.org/10.1145/3072959.3073677>
- Matt Pharr, Wenzel Jakob, and Greg Humphreys. 2021. *Physically Based Rendering, fourth edition*. The MIT Press. <https://pbr-book.org/>
- Matt Pharr, Wenzel Jakob, and Greg Humphreys. 2023. *pbrr*. <https://github.com/mmp/pbrr-v4>
- Damien Rioux-Lavoie, Joey Litalien, Adrien Gruson, Toshiya Hachisuka, and Derek Nowrouzezahrai. 2020. Delayed Rejection Metropolis Light Transport. *ACM Transactions on Graphics* 39, 3 (May 2020). <https://doi.org/10.1145/3388538>

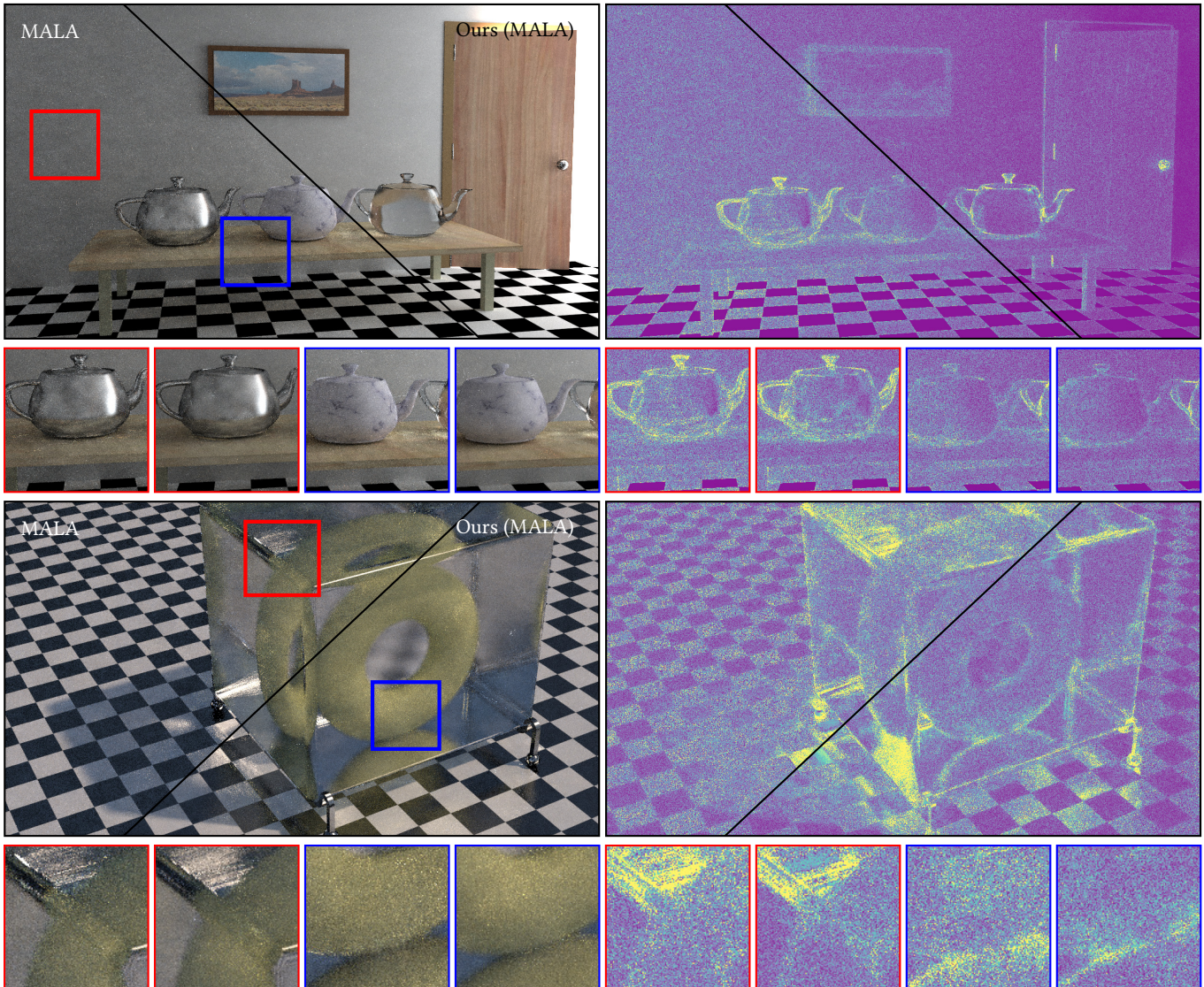


Fig. 7. We perform equal-time comparison for the MALA algorithm [Luan et al. 2020a] within our proposed framework by rendering the VEACH AJAR door scene (top) and the torus scenes (bottom). MALA is designed to better explore the local regions. When adapted to our framework, Ours (MALA) improves further upon the global discovery of the target distribution. Here the Torus scene is rendered for around 3 seconds to highlight the early improvements obtained by our framework. The improvements are directly visible in the rendered insets on the left column, but not easily spottable in the error (MAPE) images on the right.

Gareth O. Roberts and Jeffrey S. Rosenthal. 2001. Optimal scaling for various Metropolis-Hastings algorithms. *Statistical science* 16, 4 (2001).

Gareth O. Roberts and Jeffrey S. Rosenthal. 2004. General state space Markov chains and MCMC algorithms. *Probability Surveys* 1 (2004).

Michael Sharpe. 1988. *General Theory of Markov Processes*. Vol. 133. Academic Press.

Jaścha Sohl-Dickstein, Eric Weiss, Niru Maheswaranathan, and Surya Ganguli. 2015. Deep unsupervised learning using nonequilibrium thermodynamics. In *International conference on machine learning*. PMLR, 2256–2265.

Luke Tierney. 1998. A note on Metropolis-Hastings kernels for general state spaces. *The Annals of Applied Probability* 8 (1998).

Luke Tierney and Antonietta Mira. 1999. Some adaptive Monte Carlo methods for Bayesian inference. *Statistics in Medicine* 18, 17-18 (1999), 2507–2515. [https://doi.org/10.1002/\(SICI\)1097-0258\(19990915/30\)18:17/18<2507::AID-SIM272>3.0.CO;2-J](https://doi.org/10.1002/(SICI)1097-0258(19990915/30)18:17/18<2507::AID-SIM272>3.0.CO;2-J)

Eric Veach. 1997. *Robust Monte Carlo Methods for Light Transport Simulation*. Ph.D. Dissertation. Stanford University.

Eric Veach and Leonidas Guibas. 1995. Bidirectional Estimators for Light Transport. In *Photorealistic Rendering Techniques*, Georgios Sakas, Stefan Müller, and Peter Shirley (Eds.). Springer Berlin Heidelberg, Berlin, Heidelberg, 145–167.

Eric Veach and Leonidas J. Guibas. 1997. Metropolis light transport. In *Proceedings of the 24th Annual Conference on Computer Graphics and Interactive Techniques (SIGGRAPH '97)*. ACM Press/Addison-Wesley Publishing Co., USA, 65–76. <https://doi.org/10.1145/258734.258775>

Andi Q. Wang, Murray Pollock, Gareth O. Roberts, and David Steinsaltz. 2021. Regeneration-enriched Markov processes with application to Monte Carlo. *The Annals of Applied Probability* 31, 2 (2021).

A THEORETICAL CONVERGENCE INVESTIGATION

Our goal in this section is to compare the quality of an estimation based on

- (1) the Metropolis-Hastings chain M^ℓ with proposal kernel Q_ℓ and target distribution π ; and
- (2) the process X formed by the jump Restore algorithm with local dynamics M^0 and regeneration distribution μ .

The generators L_ℓ and A of M^ℓ and X will play an important role in the theoretical investigation of this comparison.

Our measure of quality will be based on the *asymptotic variance*. If $f \in L^2(\pi)$, we can define the asymptotic variance

$$\sigma_A^2(f) := \lim_{t \rightarrow \infty} \text{Var}_\pi \left[\frac{1}{\sqrt{t}} \int_0^t f(X_t) dt \right] \quad (28)$$

of the estimation (3) of πf based on X , whenever the limit exists. In that case, the ergodic average (3) is asymptotically behaving as $\sigma_A^2(f)/t$. Here, the variance is taken with respect to the probability measure with respect to which the initial distribution of X is already π . That is, the assumption in this consideration is that the process is started in stationarity.

In the $L^2(\pi)$ -reversible case, the L^2 -relaxation time [Eberle and Lörler 2024, eq. 15] of a time-homogeneous Markov process X with invariant measure π is governed by the *spectral gap*

$$\text{gap}(A) := \inf \left\{ \frac{\mathcal{F}(f)}{\|f\|_{L^2(\pi)}^2} : f \in \mathcal{D}(A) \setminus \{0\} \text{ with } \pi f = 0 \right\}. \quad (29)$$

of its $L^2(\pi)$ -generator A . Here,

$$\mathcal{F}(f, g) := -\langle Af, g \rangle_{L^2(\pi)} \quad \text{for } f \in \mathcal{D}(A) \text{ and } g \in L^2(\pi) \quad (30)$$

is the *Dirichlet form* associated with A and $\mathcal{F}(f) := \mathcal{F}(f, f)$ for $f \in \mathcal{D}(A)$. In the general, non- $L^2(\pi)$ -reversible, case, the L^2 -relaxation time is at least still lower bounded by $\text{gap}(A)$.

However, similar to the celebrated *Peskun-Tierney ordering*, we can show [Andrieu and Livingstone 2019] that an ordering

$$\mathcal{F}_\ell(f) \leq \mathcal{F}(f) \quad \text{for all } f \in \mathcal{E}_b \quad (31)$$

on the Dirichlet forms \mathcal{F}_ℓ and \mathcal{F} of X and M^ℓ , respectively, directly corresponds to an ordering

$$\sigma_{L_\ell}^2(f) \geq \sigma_A^2(f) \quad (32)$$

of the asymptotic variances of the corresponding ergodic averages.

We still can compare the performance of different processes by considering the asymptotic variances of their ergodic averages. Similar to the celebrated *Peskun-Tierney ordering* [Tierney 1998], an ordering among asymptotic variances is directly related to an ordering of the corresponding *Dirichlet forms* [Andrieu and Livingstone 2019].

That is, we can compare the asymptotic variances of M^ℓ and X by proving that their corresponding Dirichlet forms \mathcal{F}_ℓ and \mathcal{F} are ordered. We are actually able to do so:

THEOREM A.1. If

$$c_0 \geq \frac{\ell}{2p_\lambda}, \quad (33)$$

then (31) is satisfied.

PROOF: First of all, it is useful to note that

$$Q_\ell = \ell Q_1 + (1 - \ell) Q_0. \quad (34)$$

Now, the transition kernel of the Metropolis-Hastings chain $(M_n^\ell)_{n \in \mathbb{N}_0}$ is given by

$$\kappa_\ell(x, B) := \int_B Q_\ell(x, dy) \alpha_\ell(x, y) = \ell \kappa_1 + (1 - \ell) \kappa_0 \quad (35)$$

for $(x, B) \in E \times \mathcal{E}$, where α_ℓ is the acceptance function (10) of the Metropolis-Hastings algorithm with proposal kernel Q_ℓ and target density π (which effectively does not depend on ℓ , whenever the small step kernel ζ has a *symmetric* density with respect to the reference measure λ) and

$$r_\ell(x) := 1 - \int Q_\ell(x, dy) \alpha_\ell(x, y) = \ell r_1(x) + (1 - \ell) r_0 \quad (36)$$

for $x \in E$. By definition, the generator of $(M_n^\ell)_{n \in \mathbb{N}_0}$ is

$$L_\ell := \kappa_\ell - \text{id}_{\mathcal{E}_b} \quad (37)$$

and the generator of $(X_t)_{t \geq 0}$ is

$$A = L_0 + cG. \quad (38)$$

Given that, we obtain

$$\begin{aligned} \mathcal{F}(f) - \mathcal{F}_\ell(f) &= \ell \mathcal{F}_0(f) + c_0 \mathcal{G}(f) - \ell \mathcal{F}_1(f) \\ &\geq c_0 \mathcal{G}(f) - \ell \mathcal{F}_1(f) \\ &= c_0 \langle f, f - \mu f \rangle_{L^2(\mu)} \\ &\quad - \frac{\ell}{j} \pi(dy) \int \mu(dy) \alpha_\ell(x, y) |f(x) - f(y)|^2 \\ &\geq c_0 \langle f, f - \mu f \rangle_{L^2(\mu)} \\ &\quad - \frac{\ell}{2p_\lambda} \int \lambda(dx) \int \mu(dy) |f(x) - f(y)|^2 \\ &= \left(c_0 - \frac{\ell}{2p_\lambda} \right) \int \mu(dx) \int \mu(dy) |f(x) - f(y)|^2 \\ &\quad + |\mu f|^2 - \mu |f|^2 \end{aligned} \quad (39)$$

for all $f \in \mathcal{E}_b$, where

$$\mathcal{G}(f) := -\langle f, Gf \rangle_{L^2(\mu)}, \quad (40)$$

c_0 is the constant in the definition (17) of c , and λ and p_λ are defined as in subsection 3.1. Nothing that $|\mu f|^2 - \mu |f|^2$ is the variance of f with respect to the probability measure μ (hence positive for nontrivial f), the claim is immediate from this. \square